A Soluble Guanylate Cyclase–Dependent Mechanism Is Involved in the Regulation of Net Hepatic Glucose Uptake by Nitric Oxide in Vivo

Zhibo An,[1] Jason J. Winnick,[1] Ben Farmer,[1] Doss Neal,[1] Margaret Lautz,[1] Jose M. Irimia,[2] Peter J. Roach,[2] and Alan D. Cherrington[1]

OBJECTIVE—We previously showed that elevating hepatic nitric oxide (NO) levels reduced net hepatic glucose uptake (NHGU) in the presence of portal glucose delivery, hyperglycemia, and hyperinsulinemia. The aim of the present study was to determine the role of a downstream signal, soluble guanylate cyclase (sGC), in the regulation of NHGU by NO.

RESEARCH DESIGN AND METHODS—Studies were performed on 42-h–fasted conscious dogs fitted with vascular catheters. At 0 min, somatostatin was given peripherally along with 4× basal insulin and basal glucagon intraportally. Glucose was delivered at a variable rate via a leg vein to double the blood glucose level and hepatic glucose load throughout the study. From 90 to 270 min, an intraportal infusion of the sGC inhibitor 1H-[1,2,4] oxadiazolo[4,3-a] quinoxalin-1-one (ODQ) was given in −sGC (n = 10) and −sGC/+NO (n = 6), whereas saline was given in saline infusion (SAL) (n = 10). The −sGC/+NO group also received intraportal SIN-1 (NO donor) to elevate hepatic NO from 180 to 270 min.

RESULTS—In the presence of 4× basal insulin, basal glucagon, and hyperglycemia (2× basal), inhibition of sGC in the liver enhanced NHGU (mg/kg/min; 210–270 min) by ~55% (2.9 ± 0.2 in SAL vs. 4.6 ± 0.5 in −sGC). Further elevating hepatic NO failed to reduce NHGU (4.5 ± 0.7 in −sGC/+NO). Net hepatic carbon retention (i.e., glycogen synthesis; mg glucose equivalents/kg/min) increased to 3.8 ± 0.2 in −sGC and 3.8 ± 0.4 in −sGC/+NO vs. 2.4 ± 0.2 in SAL ($P < 0.05$).

CONCLUSIONS—NO regulates liver glucose uptake through a sGC-dependent pathway. The latter could be a target for pharmacologic intervention to increase meal-associated hepatic glucose uptake in individuals with type 2 diabetes. ***Diabetes*** **59: 2999–3007, 2010**

Net hepatic glucose uptake (NHGU) has been shown to be regulated by a number of factors, including the glucose load to the liver, the hepatic sinusoidal insulin level, and the negative glucose gradient between the hepatic artery and hepatic portal vein (1). When comparing the effects of peripheral versus portal venous glucose delivery on NHGU under hyperinsulinemic hyperglycemic conditions in dogs, NHGU was found to be considerably greater in the presence of intraportal glucose delivery, even when the hepatic glucose loads were well matched and insulin and glucagon levels were equivalent between groups (2–4). This suggested that a "portal glucose signal" is an important determinant of NHGU after an oral glucose load. To date, it remains unclear how the response to portal glucose delivery comes about.

In an earlier study we showed that portal but not peripheral infusion of a nitric oxide (NO) donor 3-morpholino-sydnonimine (SIN-1) reduced NHGU in the presence of portal glucose delivery, hyperglycemia, and hyperinsulinemia, suggesting that hepatic NO can regulate NHGU through a direct effect on the liver (5). This finding raised the possibility that NO may be involved in mediation of the effect of the portal glucose signal. Such speculation is supported by our finding that intraportal infusion of the nitric oxide synthase (NOS) inhibitor L-NAME enhanced NHGU under hyperinsulinemic hyperglycemic conditions in vivo (6). Further, this augmentation was partially reversed by giving SIN-1 intraportally (6). In addition, we recently found that the hepatic concentrations of nitrate and nitrite, indexes of NO levels, declined in the postprandial state in dogs (Z.A. et al., unpublished data), supporting the possibility that NO is involved in the regulation of NHGU.

The downstream consequences of NO action involve at least two distinct pathways: cyclic guanosine monophosphate (cGMP)-dependent and cGMP-independent (7). The cGMP-dependent effects result from the NO-induced activation of soluble guanylate cyclase (sGC), leading to increased cGMP levels, which modulate the activity of protein kinase G (PKG), cGMP-regulated phosphodiesterases (PDEs), and AMP-activated protein kinase (AMPK) (7). The cGMP-independent effects include S-nitrosylation and nitration of proteins (8). In addition, NO may couple with reactive oxygen species to form reactive nitrogen species such as peroxynitrite (7).

Despite the diversity of effects, it has been well documented that many metabolic actions of NO are mediated by the activation of sGC and the subsequent increase in the production of cGMP. A study in anesthetized cats showed that bolus intraportal delivery of SIN-1 potentiated norepinephrine-induced hepatic glucose output, and this potentiation was blocked by inhibition of guanylate cyclase (9). It has also been shown that blockade of hepatic NO production, or of its ability to activate guanylyl cyclase, impaired peripheral insulin sensitivity in anesthetized rodents (10,11). However, no data are available relating to the effects of sGC on hepatic glucose uptake

From the [1]Department of Molecular Physiology and Biophysics, Vanderbilt University School of Medicine, Nashville, Tennessee; and the [2]Department of Biochemistry and Molecular Biology, Indiana University School of Medicine, Indianapolis, Indiana.

Corresponding author: Zhibo An, zhibo.an@uc.edu.

Received 26 January 2010 and accepted 25 August 2010. Published ahead of print at http://diabetes.diabetesjournals.org on 7 September 2010. DOI: 10.2337/db10-0138.

under physiologic conditions. Here we test the hypothesis that a sGC-dependent mechanism is involved in the response of NHGU to hepatic NO, such that under hyperinsulinemic hyperglycemic conditions, blockade of sGC in the liver increases NHGU and prevents the reduction of NHGU caused by a rise in hepatic NO.

RESEARCH DESIGN AND METHODS

Animals and surgical procedures. Studies were performed on healthy conscious 42-h–fasted mongrel dogs of either sex with a mean weight of 21.2 ± 0.5 kg. A fast of this duration was chosen because it produces a metabolic state resembling that in the overnight-fasted human and results in liver glycogen levels in the dog that are at a stable minimum (2). All animals were maintained on a diet of meat (Pedigree, Franklin, TN) and chow (Purina Lab Canine Diet No. 5006; Purina Mills, St. Louis, MO) comprised of 34% protein, 14.5% fat, 46% carbohydrate, and 5.5% fiber based on dry weight. The animals were housed in a facility that met the American Association for Accreditation of Laboratory Animal Care guidelines, and the protocol was approved by the Vanderbilt University Medical Center Animal Care and Use Committee.

Approximately 16 days before the study, each dog underwent a laparotomy under general anesthesia (0.01 mg/kg buprenorphine before surgery, and ~1% isoflurane inhalation anesthetic during surgery), and silicone rubber sampling catheters were inserted in the hepatic vein, the portal vein, and a femoral artery as described elsewhere (2). Catheters for intraportal infusion were also placed in a splenic and a jejunal vein, while ultrasonic flow probes (Transonic Systems, Ithaca, NY) were placed around the portal vein and the hepatic artery as previously described (2).

Approximately 2 days before each study, blood was drawn to determine the leukocyte count and the hematocrit for each animal. The dog was studied only if it had a leukocyte count <18,000/mm^3, a hematocrit >35%, a good appetite (as evidenced by consumption of >75% daily ration), and normal stools.

On the morning of the study, catheters and the flow probe leads were exteriorized from their subcutaneous pockets using local anesthesia (2% lidocaine, Hospira, Lake Forest, IL). The contents of each catheter were aspirated, and catheters were flushed with saline. Angiocaths (Deseret Medical, Becton Dickinson, Sandy, UT) were inserted into the cephalic veins and the saphenous veins. Each dog was allowed to stand quietly in a Pavlov harness throughout the experiment and was studied only once.

Experimental design. As described in Fig. 1*A*, each experiment consisted of a 90-min equilibration period (−120 to −30 min), a 30-min basal period (−30 to 0 min), and a 270-min experimental period (0 to 270 min), with the latter being divided into period one (P1), 0 to 90 min, and period two (P2), 90 to 270 min. In all experiments a constant infusion of indocyanine green dye (0.076 mg/min; Sigma Immunochemicals, St. Louis, MO) was initiated at −120 min via the left cephalic vein. At the start of P1 (0 min), a constant infusion of somatostatin (0.8 μg/kg/min; Bachem, Torrance, CA) was begun via the left saphenous vein to suppress endogenous insulin and glucagon secretion. At the same time, basal glucagon (0.57 ng/kg/min; Glucagen, Novo Nordisk, Bagsvaerd, Denmark) and fourfold basal insulin (1.2 mU/kg/min; Eli Lilly & Co., Indianapolis, IN) infusions were started through the splenic and jejunal catheters (i.e., intraportally) and maintained for the duration of the study. In addition, at 0 min, a primed continuous infusion of 50% dextrose was started via the right cephalic vein so that the blood glucose could be quickly clamped at the desired hyperglycemic level (~160 mg/dl). In P2, saline was infused intraportally in the control group ([SAL], n = 10), whereas the sGC inhibitor 1H- (1,2,4) oxadiazolo[4,3-a] quinoxalin-1-one (ODQ; Cayman Chemical Company, Ann Arbor, MI) was infused intraportally at 0.8 μg/kg/min to inhibit the hepatic sGC pathway in the −sGC (n = 10) and −sGC/+NO (n = 6) groups. The NO donor SIN-1 (Cayman Chemical Company) was also infused intraportally (4 μg/kg/min) from 180 to 270 min in the −sGC/+NO group to elevate hepatic NO levels. In a separate group (+NO group; n = 3), SIN-1 was infused (4 μg/kg/min) from 90 to 270 min in the absence of ODQ. The peripheral glucose infusion rate was adjusted as needed in P2 to maintain a similar hepatic glucose load to that seen during P1.

After completion of each experiment, the animal was killed with an overdose of pentobarbital and the abdomen was opened so that the positions of the catheter tips could be verified. Liver samples were immediately freeze-clamped with precooled Wallenburger tongs and stored at −70°C for poststudy assays.

Processing and analysis of samples. The collection and immediate processing of blood samples have been described previously (12). Four to eight 10-μl aliquots of plasma from each sample were immediately analyzed for glucose using the glucose oxidase technique in a glucose analyzer (Analox Instruments, London, U.K.). Plasma insulin and glucagon concentrations were determined by radioimmunoassay, as described elsewhere (13). Cortisol, lactate, glycerol, and nonesterified fatty acid (NEFA) concentrations were also measured as previously described (14). The concentrations of hepatic cGMP were measured using a cGMP ELISA Kit (Cayman Chemical Company). Electrophoretic separation, blotting, and immunodetection of proteins were performed as described previously (15). Briefly, tissue samples were homogenized in buffer including 50 mmol/l Tris·HCl pH 7.0, 100 mmol/l sucrose, 10% (vol/vol) glycerol, 2 mmol/l EDTA, 2 mmol/l EGTA, 25 mmol/l NaF, with phosphatase and protease inhibitors (Sigma, St. Louis, MO). Homogenates were centrifuged at 10,000 g for 30 min, and supernatants were removed, mixed 1:1 (vol/vol) with 2X SDS-PAGE loading buffer (100 mmol/l Tris·HCl, pH 6.8, 4% [wt/vol] SDS, 20% [vol/vol] glycerol, 0.2% [wt/vol] bromophenol blue, 10% [vol/vol] 2-mercaptoethanol), and boiled for 10 min. Samples were then subjected to SDS-PAGE (4–12% resolving gel) followed by transfer to nitrocellulose membranes. Membranes were incubated with the appropriate primary antibody (Cell Signaling, Danvers, MA), followed by horseradish peroxidase (HRP)-conjugated secondary antibody (Promega, Madison, WI). Proteins were visualized with ECL Plus Western blotting detection reagents (GE Healthcare, Piscataway, NJ) and the ECL signal was detected after brief exposure to X-ray film. Bands were quantified with ImageJ software (http://rsb.info.nih.gov/ij). Hepatic phosphodiesterase 3 activity was determined using a modification of the phosphodiesterase assay described by Loten et al. (16), and enzyme activity (pmol ^{3}H cAMP hydrolyzed) was calculated by radioactivity counts (cpm) times 0.0000326 pmol/cpm, and normalized by protein dry weight (mg). The activities of hepatic glycogen synthase and phosphorylase were measured as described elsewhere (17,18).

Calculations and data analysis. Hepatic blood flow ([HBF] ml/kg/min) was measured using ultrasonic flow probes and by the use of indocyanine green dye according to the method of Leevy et al. (19). The results obtained with the flow probes and dye were not significantly different, but the data reported here were calculated using the former because their measurement did not require an assumption regarding the distribution of the arterial and portal vein contribution to HBF.

Net hepatic glucose balance (NHGB; mg/kg/min) was calculated as:

$$\mathrm{NHGB} = \mathrm{Load}_{out} - \mathrm{Load}_{in}.$$

$$\mathrm{Load}_{in} = (G_A \times \mathrm{ABF}) + (G_P \times \mathrm{PBF}).$$

Where G_A (mg/ml) is the arterial blood glucose concentration, G_P (mg/ml) is the portal blood glucose concentration, ABF (ml/kg/min) is hepatic arterial blood flow, and PBF (ml/kg/min) is hepatic portal blood flow.

The load of glucose exiting the liver was calculated as:

$$\mathrm{Load}_{out} = (G_H \times \mathrm{HBF}).$$

Where G_H (mg/ml) represents the hepatic vein glucose concentration and HBF = ABF + PBF.

The average nonhepatic glucose uptake between two time points (T1 and T2) was calculated by subtracting the rate of NHGU and the change in the glucose mass from the total glucose infusion rate using the equation: nonhepatic glucose uptake rate = average total glucose infusion rate between T1 and T2 − (NHGU_{T1} + NHGU_{T2})/2 − the change in the glucose mass between T1 and T2. In a previous study, we were able to determine that under hyperinsulinemic and hyperglycemic conditions, virtually all the increase in nonhepatic glucose uptake could be accounted for muscle glucose uptake (12). Net hepatic carbon retention was calculated as the sum of the net balances of glucose and lactate once the latter was converted to glucose equivalents (5). The calculation of net hepatic carbon retention is an established approach to estimate hepatic glycogen accretion and has been described and validated previously (20). Although the calculation omits the contribution of gluconeogenic substrates other than lactate and fails to account for glucose oxidized by the liver, these two rates are quantitatively similar and offsetting. Net hepatic fractional glucose extraction was calculated as the ratio of NHGB to Load_{in}. The net hepatic balances of lactate, glycerol, and NEFA were calculated as for glucose. The hepatic sinusoidal insulin and glucagon concentrations were calculated as described elsewhere (21).

For all glucose balance calculations, glucose concentrations were converted from plasma to blood values by using previously determined (22,23) conversion factors (CF: the mean of the ratio of the blood value to the plasma concentration). The use of whole blood glucose values ensures accurate hepatic balance measurements regardless of the characteristics of glucose entry into the erythrocyte.

Statistical analysis. All data are presented as means ± SEM. Time course data were analyzed with two-way repeated measures ANOVA, and one-way ANOVA was used for comparisons of other mean data. Post hoc analysis was performed using the Student-Newman-Keuls method. Statistical significance was accepted at $P < 0.05$.

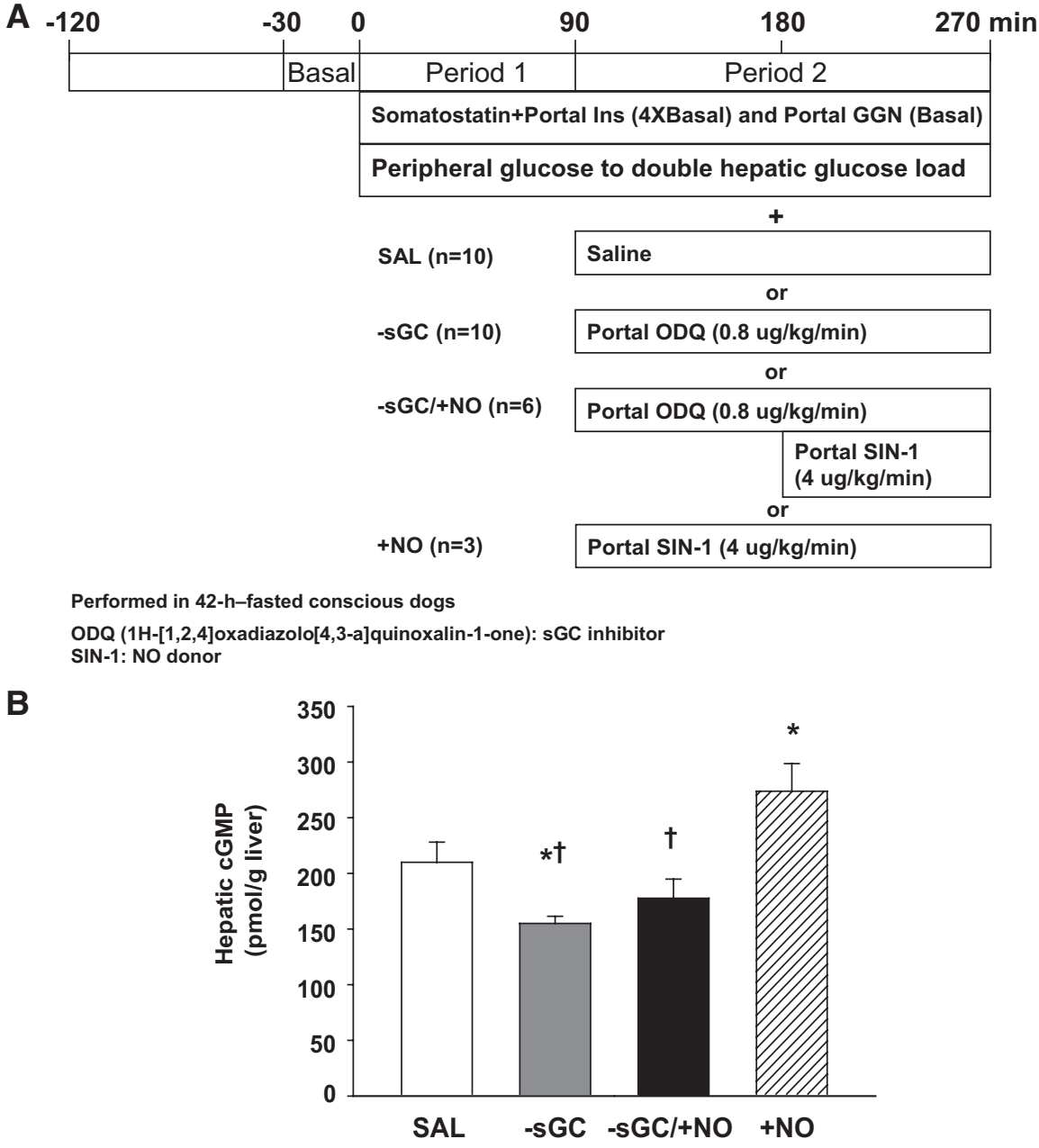

FIG. 1. Schematic representation of the study (*A*) and hepatic cGMP levels (*B*). The protocol comprises the basal (−30 to 0 min) and experimental periods (period 1: 0–90 min; period 2: 90–270 min). Somatostatin was infused peripherally and insulin (fourfold basal) and glucagon (basal) were given intraportally, whereas glucose was delivered peripherally at a variable rate to increase the hepatic glucose load twofold basal during period 1 and period 2. Data are means ± SEM. **P* < 0.05 compared with the SAL group. †*P* < 0.05 compared with the +NO group.

RESULTS

Inhibition of cGMP levels in the liver. To verify the inhibition of sGC in the liver, hepatic cGMP levels were measured in biopsies taken at the end of the experiments. Relative to saline infusion (SAL), intraportal infusion of the sGC inhibitor ODQ (−sGC) led to a decrease of 26% in hepatic cGMP levels, (Fig. 1*B*) whereas SIN-1 alone (+NO) increased cGMP levels in the liver by 31%. ODQ effectively blocked the ability of the NO donor to elevate cGMP levels.

Hormone concentrations. During the hyperinsulinemic hyperglycemic clamp (P1 and P2), the arterial and hepatic sinusoidal insulin levels quickly increased three to fourfold and remained stable thereafter (Table 1). Arterial and hepatic sinusoidal plasma glucagon concentrations, on the other hand, remained basal throughout the study in all groups, as did the arterial plasma cortisol concentrations (Table 1).

Hepatic blood flow, blood glucose concentrations, and hepatic glucose load. Portal vein blood flow decreased ~20% in all groups in response to somatostatin infusion (Table 2). There was a concomitant and partly offsetting (~10–20%) increase in hepatic arterial flow. Consequently, total hepatic blood flow tended to be reduced slightly (~10%) during the experimental period, but it was unaffected by ODQ or SIN-1 infusion.

During the hyperglycemic clamp, arterial blood glucose levels increased in all the groups from a basal value of ~80 to ~160 mg/dl (Fig. 2*A*, Table 3). The hepatic glucose loads

TABLE 1
Average hormone concentrations during the basal and experimental periods in conscious 42-h–fasted dogs given saline, ODQ, ODQ + SIN-1, or SIN-1 into the portal vein

Group	Basal period	Experimental period	
		Period 1	Period 2
Arterial plasma insulin, μU/ml			
SAL	8 ± 1	20 ± 2*	23 ± 2*
−sGC	7 ± 1	20 ± 2*	22 ± 2*
−sGC/+NO	6 ± 1	18 ± 2*	21 ± 2*
+NO	7 ± 2	18 ± 1*	21 ± 2*
Hepatic sinusoidal insulin, μU/ml			
SAL	23 ± 3	85 ± 12*	83 ± 8*
−sGC	24 ± 5	80 ± 8*	85 ± 10*
−sGC/+NO	19 ± 3	89 ± 8*	83 ± 6*
+NO	25 ± 3	88 ± 20*	82 ± 9*
Arterial plasma glucagon, pg/ml			
SAL	39 ± 4	39 ± 3	36 ± 4
−sGC	41 ± 4	40 ± 4	38 ± 3
−sGC/+NO	33 ± 4	35 ± 4	35 ± 3
+NO	43 ± 2	46 ± 12	43 ± 9
Hepatic sinusoidal glucagon, pg/ml			
SAL	44 ± 6	52 ± 4	49 ± 5
−sGC	47 ± 7	53 ± 6	54 ± 5
−sGC/+NO	40 ± 6	50 ± 3	47 ± 3
+NO	47 ± 3	61 ± 7	56 ± 8
Arterial cortisol, μg/dl			
SAL	4 ± 1	4 ± 1	3 ± 1
−sGC	4 ± 1	4 ± 1	2 ± 1
−sGC/+NO	4 ± 1	3 ± 1	3 ± 1
+NO	6 ± 4	4 ± 2	4 ± 2

Data are means ± SEM; $n = 10$ in SAL and −sGC groups. $n = 6$ in the −sGC/+NO group. $n = 3$ in the + NO group. *Significant statistical difference ($P < 0.05$) from basal period within the group. Basal period: −30 to 0 min; experimental period 1: 0–90 min; period 2: 90–270 min.

TABLE 2
Average hepatic arterial, portal, and total hepatic blood flow during the basal and experimental periods in conscious 42-h–fasted dogs given saline, ODQ, ODQ + SIN-1, or SIN-1 into the portal vein

Group	Basal period	Experimental period	
		Period 1	Period 2
Average hepatic arterial blood flow, ml/kg/min			
SAL	5.4 ± 0.4	6.4 ± 0.5	7.3 ± 0.8*
−sGC	6.1 ± 0.8	7.8 ± 1.1	8.6 ± 1.0*
−sGC/+NO	5.0 ± 0.4	5.0 ± 0.4	5.7 ± 0.4
+NO	4.7 ± 1.3	4.3 ± 0.6	5.2 ± 0.8
Average hepatic portal blood flow, ml/kg/min			
SAL	24.1 ± 2.0	19.4 ± 1.9*	18.4 ± 1.8*
−sGC	26.4 ± 2.4	20.0 ± 2.2*	20.1 ± 2.0*
−sGC/+NO	23.3 ± 3.2	18.3 ± 2.2	19.5 ± 2.3
+NO	21.5 ± 4.3	17.2 ± 4.1	20.3 ± 3.1
Average total hepatic blood flow, ml/kg/min			
SAL	29.5 ± 2.1	25.8 ± 2.1	25.7 ± 2.1
−sGC	32.5 ± 2.8	27.7 ± 3.0	28.7 ± 2.6
−sGC/+NO	28.3 ± 3.5	23.3 ± 2.4	25.2 ± 2.5
+NO	26.2 ± 3.9	21.5 ± 3.5	25.5 ± 2.3

Data are means ± SEM; $n = 10$ in SAL and −sGC groups. $n = 6$ in the −sGC/+NO group. $n = 3$ in the + NO group. *Significant statistical difference ($P < 0.05$) from basal period within the group.

increased proportionally and did not differ among groups (Fig. 2*B*, Table 3).

Net hepatic glucose balance and net hepatic fractional glucose extraction. All groups exhibited a similar rate of net hepatic glucose output during the basal period. Coincident with the start of the experimental period (4× basal insulin, basal glucagon, and hyperglycemia), all groups switched from net output to net uptake of glucose, and the rates (2.3 ± 0.3, 2.2 ± 0.3, and 2.5 ± 0.4 mg/kg/min in SAL, −sGC, and −sGC/+NO, respectively) did not differ among the groups (Fig. 2*C*). During the last hour of the experiment, NHGU was 2.9 ± 0.2 mg/kg/min in SAL and 4.6 ± 0.5 and 4.5 ± 0.7 mg/kg/min ($P < 0.05$ vs. SAL) in −sGC and −sGC/+NO, respectively. The net hepatic fractional extraction of glucose followed a similar pattern, increasing similarly in response to the inhibition of sGC, even when the NO donor, SIN-1, was present (Fig. 2*D*). Infusing SIN-1 in the absence of ODQ (+NO; Table 3) had no effect on NHGU (2.8 ± 0.8 mg/kg/min during the last hour of the experiment; Table 3). Taken together, the above data suggest that a decrease in hepatic cGMP brings about an increase in NHGU. Further, since SIN-1 could not reduce NHGU when hepatic sGC was inhibited, it appears that NO brings about its effect through this mechanism.

Glucose infusion rates and nonhepatic glucose uptake. The glucose infusion and nonhepatic glucose uptake rates increased over time in all groups (Fig. 2*E*, Table 3). In the −sGC and −sGC/+NO groups, the glucose infusion rates were significantly increased over that required in the saline and +NO group. Nonhepatic glucose uptake did not differ significantly between groups at any time, although there was a tendency for it to be increased in the presence of ODQ (Fig. 2*F*, Table 3).

Lactate metabolism and net hepatic carbon retention. The arterial blood lactate concentrations rose in all groups during P1 and P2 (Table 4). After the experimental period began, net hepatic lactate balance changed from uptake to output, and this continued in all groups during P2 (Table 4). An index of hepatic glycogen accretion, net hepatic carbon retention (mg glucose equivalents/kg/min), did not differ among groups during P1 (1.8 ± 0.3, 1.4 ± 0.6, 1.9 ± 0.3, and 1.8 ± 0.2 in SAL, +NO, −sGC, and −sGC/+NO. respectively) but was increased ($P < 0.05$) relative to the SAL and +NO group during P2 in response to sGC inhibition, regardless of the presence or absence of SIN-1 (2.4 ± 0.2 in SAL, 2.3 ± 0.5 in +NO vs. 3.8 ± 0.2 in −sGC and 3.8 ± 0.4 in −sGC/+NO).

Glycerol and nonesterified fatty acid metabolism. Arterial blood glycerol concentrations and net hepatic glycerol uptake were reduced by 55 to 70% in response to hyperinsulinemia and remained suppressed in all groups during P1 (Table 4). The suppression of glycerol was, however, partially reversed during P2 in the +NO but not SAL, −sGC, and −sGC /+NO groups (Table 4). This is

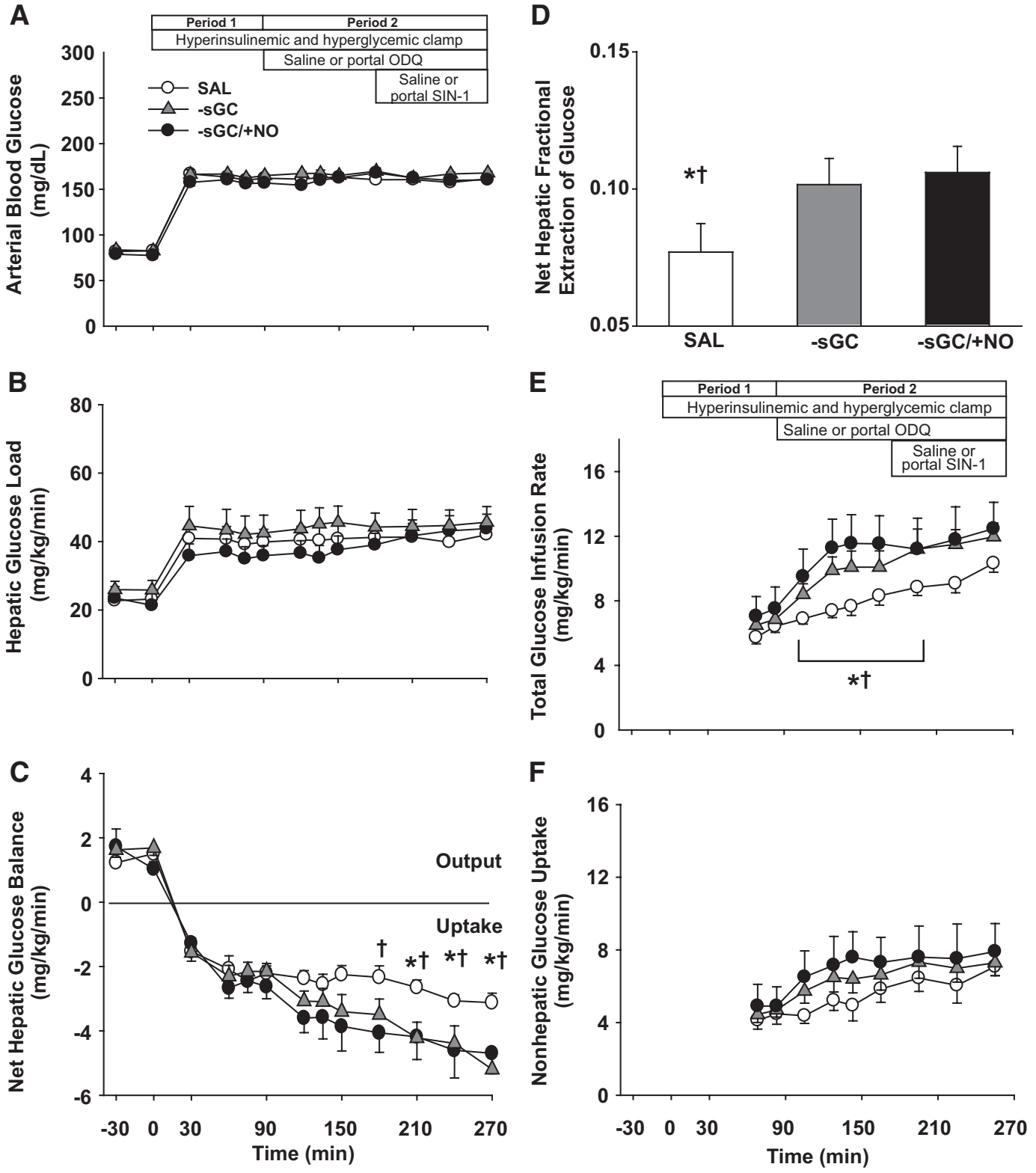

FIG. 2. Arterial blood glucose (*A*), hepatic glucose loads (*B*), net hepatic glucose uptake (*C*), net hepatic fractional extraction of glucose (*D*), glucose infusion rate (*E*), and nonhepatic glucose uptake (*F*) in 42-h–fasted conscious dogs during the basal and experimental periods. See Fig. 1*A* for description of study conditions. Data are means ± SEM. Net hepatic fractional extraction of glucose data represent the averaged values for the last hour in each group. **P* < 0.05 compared with the −sGC group. †*P* < 0.05 compared with the −sGC/+NO group.

consistent with our previous observation that intraportal SIN-1 resulted in a rebound of lipolysis under hyperinsulinemic hyperglycemic conditions (5). This effect was blocked in the present study when ODQ was given at the same time. Arterial plasma NEFA concentrations and net hepatic NEFA uptake changed in a pattern similar to glycerol (Table 4).

Glycogen metabolism and insulin signaling in the liver. In agreement with net hepatic carbon retention data, the hepatic glycogen content at the end of the

TABLE 3
Average arterial glucose, hepatic glucose load, total glucose infusion rate, and nonhepatic glucose uptake during the basal and experimental periods in conscious 42-h–fasted dogs given SIN-1 (the +NO group) into the portal vein

		Experimental period	
Parameters	Basal period	Period 1	Period 2
Arterial blood glucose, mg/dl	80 ± 6	161 ± 2*	159 ± 4*
Hepatic glucose load, mg/kg/min	19 ± 2	34 ± 6*	40 ± 4*
Net hepatic glucose balance, mg/kg/min	1.5 ± 0.2	−1.8 ± 0.9*	−2.8 ± 0.8*
Total glucose infusion rate, mg/kg/min	0	4.8 ± 0.4	6.8 ± 0.4
Nonhepatic glucose uptake, mg/kg/min	1.5 ± 0.2	3.4 ± 0.7	4.4 ± 0.9

Data are means ± SEM; $n = 3$. *Significant statistical difference ($P < 0.05$) from basal period. Negative values for balance data indicate net hepatic uptake.

TABLE 4
Average lactate, glycerol, and NEFA concentration and net hepatic balance during the basal and experimental periods in conscious 42-h–fasted dogs given saline, ODQ, ODQ + SIN-1, or SIN-1 into the portal vein

		Experimental period	
Group	Basal period	Period 1	Period 2
Arterial blood lactate, μmol/l			
SAL	506 ± 119	966 ± 72	852 ± 62
−sGC	461 ± 52	1,033 ± 144	909 ± 99
−sGC/+NO	438 ± 61	848 ± 122	866 ± 124
+NO	432 ± 111	903 ± 162	854 ± 141
Net hepatic lactate balance, μmol/kg/min			
SAL	−6.0 ± 1.1	4.8 ± 1.0	3.5 ± 1.1
−sGC	−5.4 ± 1.4	5.3 ± 1.8	3.0 ± 1.2
−sGC/+NO	−4.9 ± 0.9	8.0 ± 2.6	6.3 ± 1.9
+NO	−6.1 ± 0.7	5.5 ± 3.6	3.1 ± 2.2
Arterial blood glycerol, μmol/l			
SAL	84 ± 8	38 ± 7	35 ± 6
−sGC	88 ± 9	37 ± 7	29 ± 6
−sGC/+NO	74 ± 14	29 ± 7	31 ± 8
+NO	82 ± 12	38 ± 13	63 ± 21
Net hepatic glycerol uptake, μmol/kg/min			
SAL	1.2 ± 0.2	0.4 ± 0.1	0.5 ± 0.1
−sGC	1.8 ± 0.2	0.5 ± 0.2	0.6 ± 0.2
−sGC/+NO	1.4 ± 0.2	0.5 ± 0.1	0.6 ± 0.2
+NO	1.4 ± 0.3	0.6 ± 0.4	1.1 ± 0.5
Arterial plasma NEFA, μmol/l			
SAL	949 ± 106	154 ± 36	127 ± 29
−sGC	955 ± 96	140 ± 27	146 ± 39
−sGC/+NO	883 ± 161	101 ± 21	121 ± 33
+NO	990 ± 136	332 ± 108	285 ± 91
Net hepatic NEFA uptake, μmol/kg/min			
SAL	2.1 ± 0.4	0.3 ± 0.1	0.3 ± 0.2
−sGC	2.7 ± 0.4	0.3 ± 0.1	0.4 ± 0.2
−sGC/+NO	2.1 ± 0.4	0.3 ± 0.1	0.4 ± 0.2
+NO	3.7 ± 1.4	1.7 ± 1.0	1.6 ± 0.8

Data are means ± SEM; $n = 10$ in SAL and −sGC groups. $n = 6$ in the −sGC/+NO group. $n = 3$ in the +NO group. All values in each group during the experimental period are significantly different ($P < 0.05$) from the basal period. Negative values for balance data indicate net hepatic uptake.

experiment (only measured in SAL and −sGC) was greater following the inhibition of sGC (SAL vs. −sGC; Table 5). However, hepatic glycogen synthase and phosphorylase activities were not different between the two groups (Table 5). Phosphorylation of hepatic AKT and GSK-3 β in the liver also did not differ between the two groups (Table 5).

AMP-activated protein kinase signaling and phosphodiesterase 3 activity in the liver. Compared with the saline group, intraportal infusion of ODQ was associated with a decrease of ~30% in the phosphorylation of phospho-AMPKα (Thr172) in the liver as well in the phosphorylation of Ser-79 in its downstream target acetyl-CoA carboxylase (ACC) (Fig. 3). In contrast, intraportal SIN-1 alone, which elevated hepatic NO, was associated with a ~25% increase in phospho AMPK and a ~30% increase in phospho ACC (Fig. 3). ODQ blocked the effect of the NO donor SIN-1 on the phosphorylation of both AMPK and ACC. PDE3 (cGMP-inhibited cAMP phosphodiesterase) activity (pmol/min/mg dry weight) was not altered by inhibition of hepatic sGC ($3.6 \times 10^{-3} \pm 0.3 \times 10^{-3}$ in ODQ vs. $3.2 \times 10^{-3} \pm 0.3 \times 10^{-3}$ in SAL).

DISCUSSION

To our knowledge, this is the first in vivo work that assessed the effects of the sGC pathway on glucose uptake by the liver under hyperinsulinemic hyperglycemic conditions. Under these conditions, inhibition of sGC in the liver caused an ~50% increase in NHGU and hepatic glycogen accumulation. Simultaneous elevation of hepatic NO was not able to override the enhancement of NHGU induced by sGC inhibition, suggesting that NO brings about its effect through a sGC-dependent mechanism. Furthermore, the correspondence between hepatic cGMP content and hepatic AMPK activation raises the possibility that the latter may be involved in the regulation of NHGU by this pathway.

Our previous study showed that under hyperglycemic, hyperinsulinemic conditions and in the presence of portal glucose delivery, portal but not peripheral infusion of the NO donor SIN-1 inhibited NHGU, suggesting that the effect of NO was the result of a direct effect within the liver (5). The three isoforms of NOS are expressed within the liver (24–26), and NO infusion (~0.15 μmol/g liver/min) has been shown to activate glycogen breakdown in the perfused rat liver (27). Likewise, Sprangers et al. (28) showed that glycogen synthesis in rat hepatocytes was inhibited by the NO donor S-nitroso-N-acetylpenicillamine (SNAP). The current study extends these earlier results by providing data to support the concept that sGC can regulate NHGU in vivo under physiologic hyperinsulinemic, hyperglycemic conditions.

We chose ODQ as the tool to study the role of sGC in the present study because it is considered to be the most specific sGC inhibitor available (29). The cGMP data clearly show that the drug hit its target. As with any chemical blocker, however, one must consider whether it might have caused a change through an off-target effect (30). This seems unlikely in the present case for several

TABLE 5
Postexperimental hepatic glycogen, glycogen synthase, and phosphorylase activities, Akt, and GSK-3β in conscious 42-h–fasted dogs given saline or ODQ into the portal vein

Group	Value at the end of the experiments
Terminal hepatic glycogen content (mg/g liver)	
SAL	23 ± 3
−sGC	34 ± 2*
Hepatic glycogen synthase activity ratio (L/H)	
SAL	0.09 ± 0.01
−sGC	0.09 ± 0.01
Hepatic glycogen phosphorylase activity ratio (−/+ AMP)	
SAL	0.12 ± 0.02
−sGC	0.12 ± 0.01
Hepatic phospho Akt/total Akt ratio	
SAL	0.87 ± 0.19
−sGC	0.89 ± 0.11
Hepatic phospho GSK-3β/total GSK-3β ratio	
SAL	0.85 ± 0.12
−sGC	0.89 ± 0.17

Data are means ± SEM; $n = 10$ in SAL and −sGC groups. In the presence of basal insulin, hepatic glycogen synthase activity ratio (L/H) is ~0.02, glycogen phosphorylase activity ratio (−/+ AMP) is ~0.20, P-Akt/total Akt is ~0.22 and P-GSK-3β/Total GSK-3βis ~0.25. *Significant statistical difference ($P < 0.05$) from the SAL group.

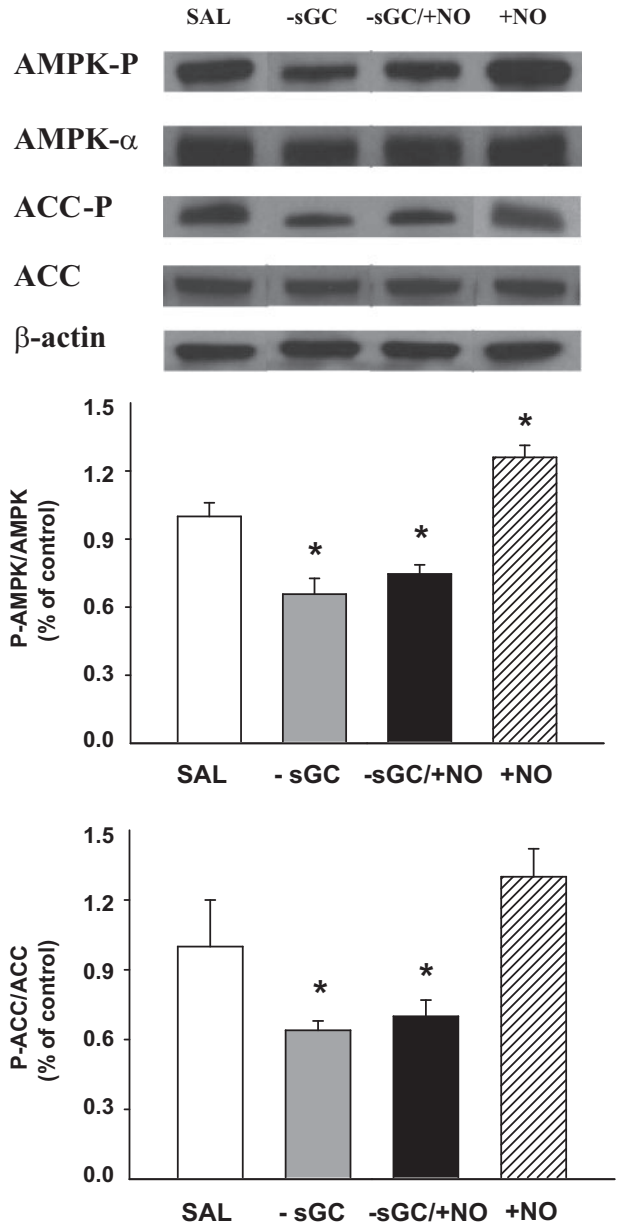

FIG. 3. Phosphorylation of AMPK at Thr172 and ACC at Ser79 in the liver biopsies at the end of the experiments. See Fig. 1*A* for a description of study conditions. Data are means ± SEM; *$P < 0.05$ compared with the SAL group. The blots shown are representative of 3 to 5 blots obtained from independent experiments.

reasons. First, we have preliminary data that show that intraportal infusion of 8-Bromo cGMP inhibits NHGU in the dog (31), thereby supporting the role of sGC in the regulation of NHGU. Moreover, the dose of ODQ (0.8 μg/kg/min) that we used in the present study would have produced ODQ levels markedly below those having been shown to have off-target effects (100 μmol/l) in a 10C9 B cell line (30). If we assume that all of the infused drug accumulated in plasma (no binding or elimination), then the level reached by the time NHGU was significantly increased (180 min) would have been ~7 μmol/l. Since some of the drug must have been cleared over the 90-min infusion period, its plasma concentration was probably closer to two orders of magnitude less than those shown to have off-target effects (30).

There are several possible ways that hepatic NO/sGC/cGMP could affect NHGU. Many of the biologic effects of NO are mediated by PKG (32), so it is possible that a PKG-dependent pathway produces the downstream signal controlling NHGU. However, PKG levels in the liver are very low, and very few hepatic metabolic enzymes have been identified as physiologic targets of PKG (33,34). It has also been well established that cAMP leads to activation of cAMP-dependent protein kinase (PKA), which in turn phosphorylates enzymes involved in the regulation of glycogen metabolism, gluconeogenesis, and glycolysis (35). Since cGMP inhibits PDE3, which hydrolyzes cAMP, it is conceivable that inhibition of hepatic sGC could lower hepatic cGMP, thereby removing the inhibition on PDE3, which could, in turn, reduce hepatic cAMP levels and potentially increase liver glucose uptake. However, the PDE3 activity in the liver was not different following the inhibition of sGC, suggesting that PDE3 was not responsible for the metabolic response seen in the present study. In addition, we found that Akt phosphorylation was unchanged in the liver in response to the change of hepatic sGC/cGMP, suggesting that the regulation of NHGU by NO is not likely caused by a modification in the insulin-signaling cascade.

It is also possible that NO/sGC/cGMP regulates NHGU through the AMPK pathway. The phosphorylation and activation of AMPK is catalyzed by upstream AMPK kinases, such as LKB1 and calmodulin-dependent protein kinase kinase (CaMKK), as well as allosteric activation via AMP binding (36). NO may increase AMPK activity via activation of AMPK kinases and/or inhibition of protein phosphatases responsible for AMPK dephosphorylation (37). It has recently been reported that NO can activate AMPK in endothelium via a sGC/cGMP-dependent path-

way by increasing intracellular Ca^{2+} and subsequently activating CaMKK (37,38). In snail muscle, 8-Bromo cGMP, a cGMP analog, activates AMPK (39). In line with this concept, in the present study, inhibition of hepatic sGC was associated with a decrease (~30%) in the phosphorylation of Thr172 in hepatic AMPK with no change in its protein level. This observation is confirmed by a reduction in the phosphorylation of ACC, a downstream marker of AMPK activity, in the liver.

AMPK has been proposed to act as a "metabolic master switch" mediating the adaptation to the cellular energy status. It has also been implicated in the control of hepatic glucose homeostasis (40), although the findings are not all consistent. Bergeron et al. (41) showed that systemic infusion of 5′-aminoimidazole-4-carboxamide-1-β-D-ribofuranoside (AICAR), an AMPK activator, suppressed hepatic glucose output in overnight-fasted normal and obese rats. This finding was supported by the observation that a constitutively active form of AMPKα2 reduced glucose output in cultured hepatocytes (42) and the in vivo observation that liver-specific *AMPKα2* KO mice had increased fasting hepatic glucose production (43). These results were in contrast, however, to those of Iglesias et al. (44) who showed that an intraperitoneal injection of AICAR caused a marked increment in net hepatic glycogen breakdown in 5-h–fasted rats. In agreement with this finding, Camacho et al. (45) and Pencek et al. (46) showed that intraportal AICAR infusion in 18-h–fasted conscious dogs led to an increase in hepatic glucose output in the presence of basal glucagon, high physiologic insulin, and either hyperglycemia, euglycemia, or hypoglycemia. These authors also showed that the increase in hepatic glucose output in response to AICAR infusion was caused by a stimulation of hepatic glycogenolysis. The latter observation is in line with the suggestion that AMPK can inactivate glycogen synthase and activate phosphorylase (47). Furthermore, a recent observation showed that AMPK activation inhibited glucose phosphorylation and glucokinase translocation in hepatocytes (48); therefore, inactivation of AMPK in the liver could promote NHGU by augmenting glucokinase translocation. Although the current study shows that reductions in AMPK phosphorylation correlated with reductions in hepatic cGMP levels, it remains to be proven that AMPK is the link between enhanced NHGU and sGC inhibition. Further studies in which AMPK is activated or inhibited under hyperglycemic, hyperinsulinemic conditions will be needed to prove causality.

Although there was an ~50% increase in hepatic glycogen accumulation after the inhibition of sGC in the liver, it is interesting to note that neither hepatic glycogen synthase nor phosphorylase activities changed in response to the inhibition of sGC. This is probably due to the fact that the in vitro synthase and phosphorylase assays do not reflect the allosteric regulation of the activities of these enzymes which occurs in vivo and which may be enhanced during sGC inhibition in the liver.

We previously showed that intraportal SIN-1 reduced NHGU in the presence of portal glucose delivery, hyperglycemia, and hyperinsulinemia in conscious dogs (5). Likewise, intraportal infusion of the NOS inhibitor L-NAME enhanced NHGU under hyperinsulinemic hyperglycemic conditions in the absence of portal glucose delivery, and this augmentation was partially reversed by giving SIN-1 intraportally (6). In the present study, we found that an increase in hepatic NO induced by SIN-1 infusion (+NO group) failed to reduce NHGU significantly when the portal glucose signal was absent, suggesting that an increase in NO is not able to inhibit NHGU when hepatic glucose uptake is not activated by a negative arterial portal glucose gradient. The present results, combined with our earlier findings, thus raise the possibility that the hepatic NO/sGC/cGMP pathway produces a basal inhibitory signal which limits NHGU during fasting. Further, we postulate that the removal of this signal by feeding causes a decrease in NO, a decrease in hepatic cGMP, and an increase in liver glucose uptake. Modulation of nitrergic signaling in the liver may explain at least part of the effect of the portal glucose signal on hepatic glucose uptake.

In conclusion, we demonstrate for the first time that the inhibition of sGC in the liver in vivo increases net hepatic glucose uptake and hepatic glycogen synthesis under hyperinsulinemic hyperglycemic conditions in conscious 42-h–fasted dogs. These data raised the possibility that the NO/sGC/cGMP pathway is involved in the regulation of liver glucose uptake during feeding, making it a potentially useful target for the treatment of type 2 diabetes.

ACKNOWLEDGMENTS

This research was supported by the National Institutes of Health grant RO1 DK-43706. Hormone analysis was performed by the Hormone Assay & Analytical Services Core, Vanderbilt Diabetes Research and Training Center, supported by National Institutes of Health grant P60 DK-020593.

No potential conflicts of interest relevant to this article were reported.

Z.A. researched data, wrote the manuscript, and reviewed/edited the manuscript. J.J.W. and J.M.I. researched data and reviewed/edited the manuscript. B.F., D.N., and M.L. researched data. P.J.R. contributed to discussion and reviewed/edited the manuscript. A.D.C. researched data, contributed to discussion, and reviewed/edited the manuscript.

This work was presented, in part, at the 44th annual meeting of the European Association for the Study of Diabetes, Rome, Italy, September 2008. A.D.C. is the Jacquelyn A. Turner and Dr. Dorothy J. Turner Chair in Diabetes Research.

The authors appreciate the assistance and support of Jon Hastings and Patsy Raymer and a critical reading of this manuscript by Dr. Mary C. Moore, Dr. Dale S. Edgerton, Dr. Chris J. Ramnanan, and Katie Coate, Vanderbilt University. The authors would also like to thank Phil Williams for technical assistance.

REFERENCES

1. Cherrington AD. Banting Lecture 1997. Control of glucose uptake and release by the liver in vivo. Diabetes 1999;48:1198–1214
2. Adkins-Marshall BA, Myers SR, Hendrick GK, Williams PE, Triebwasser K, Floyd B, Cherrington AD. Interaction between insulin and glucose-delivery route in regulation of net hepatic glucose uptake in conscious dogs. Diabetes 1990;39:87–95
3. Myers SR, McGuinness OP, Neal DW, Cherrington AD. Intraportal glucose delivery alters the relationship between net hepatic glucose uptake and the insulin concentration. J Clin Invest 1991;87:930–939
4. Pagliassotti MJ, Cherrington AD. Regulation of net hepatic glucose uptake in vivo. Annu Rev Physiol 1992;54:847–860
5. An Z, DiCostanzo CA, Moore MC, Edgerton DS, Dardevet DP, Neal DW, Cherrington AD. Effects of the nitric oxide donor SIN-1 on net hepatic glucose uptake in the conscious dog. Am J Physiol Endocrinol Metab 2008;294:E300–E306
6. Moore MC, DiCostanzo CA, Farmer B, Smith MS, Snead WL, Cherrington AD. Portal delivery of a nitric oxide synthase inhibitor enhances net hepatic glucose uptake in the conscious dog. Diabetologia 2005;48:A228

7. Ziolo MT, Kohr MJ, Wang H. Nitric oxide signaling and the regulation of myocardial function. J Mol Cell Cardiol 2008;45:625–632.
8. Stamler JS, Lamas S, Fang FC. Nitrosylation. the prototypic redox-based signaling mechanism. Cell 2001;106:675–683
9. Ming Z, Han C, Lautt WW. Nitric oxide inhibits norepinephrine-induced hepatic vascular responses but potentiates hepatic glucose output. Can J Physiol Pharmacol 2000;78:36–44
10. Sadri P, Lautt WW. Blockade of hepatic nitric oxide synthase causes insulin resistance. Am J Physiol 1999;277:G101–G108
11. Correia NC, Guarino MP, Raposo J, Macedo MP. Hepatic guanylyl cyclase inhibition induces HISS-dependent insulin resistance. Proc West Pharmacol Soc 2002;45:57–58
12. Galassetti P, Shiota M, Zinker BA, Wasserman DH, Cherrington AD. A negative arterial-portal venous glucose gradient decreases skeletal muscle glucose uptake. Am J Physiol 1998;275:E101–E111
13. Morgan CR, Lazarow A. Immunoassay of insulin using a two-antibody system. Proc Soc Exp Biol Med 1962;110:29–32
14. Moore MC, Rossetti L, Pagliassotti MJ, Monahan M, Venable C, Neal D, Cherrington AD. Neural and pancreatic influences on net hepatic glucose uptake and glycogen synthesis. Am J Physiol 1996;271:E215–E222
15. Winnick JJ, An Z, Moore MC, Ramnanan CJ, Farmer B. A physiological increase in the hepatic glycogen level does not affect the response of net hepatic glucose uptake to insulin. Am J Physiol Endocrinol Metab 2009; 297:E358–E366.
16. Loten EG, Francis SH, Corbin JD. Proteolytic solubilization and modification of hormone-sensitive cyclic nucleotide phosphodiesterase. J Biol Chem 1980;255:7838–7844
17. Gilboe DP, Larson KL, Nuttall FQ. Radioactive method for the assay of glycogen phosphorylases. Anal Biochem 1972;47:20–27
18. Guinovart JJ, Salavert A, Massague J, Ciudad CJ, Salsas E, Itarte E. Glycogen synthase: a new activity ratio assay expressing a high sensitivity to the phosphorylation state. FEBS Lett 1979;106:284–288
19. Leevy CM, Mendenhall CL, Lesko W, Howard MM. Estimation of hepatic blood flow with indocyanine green. J Clin Invest 1962;41:1169–1179
20. Satake S, Moore MC, Igawa K, Converse M, Farmer B, Neal DW, Cherrington AD. Direct and indirect effects of insulin on glucose uptake and storage by the liver. Diabetes 2002;51:1663–1671
21. Edgerton DS, Lautz M, Scott M, Everett CA, Stettler KM, Neal DW, Chu CA, Cherrington AD. Insulin's direct effects on the liver dominate the control of hepatic glucose production. J Clin Invest 2006;116:521–527
22. Hsieh PS, Moore MC, Neal DW, Cherrington AD. Hepatic glucose uptake rapidly decreases after removal of the portal signal in conscious dogs. Am J Physiol 1998;275:E987–E992
23. Moore MC, Hsieh PS, Flakoll PJ, Neal DW, Cherrington AD. Differential effect of amino acid infusion route on net hepatic glucose uptake in the dog. Am J Physiol 1999;276:E295–E302
24. Alexander B. The role of nitric oxide in hepatic metabolism. Nutrition 1998;14:376–390
25. Feelisch M, Kotsonis P, Siebe J, Clement B, Schmidt HH. The soluble guanylyl cyclase inhibitor 1H-(1,2,4)oxadiazolo[4,3,-a] quinoxalin-1-one is a nonselective heme protein inhibitor of nitric oxide synthase and other cytochrome P-450 enzymes involved in nitric oxide donor bioactivation. Mol Pharmacol 1999;56:243–253
26. Wei CL, Khoo HE, Lee KH, Hon WM. Differential expression and localization of nitric oxide synthases in cirrhotic livers of bile duct-ligated rats. Nitric Oxide 2002;7:91–102
27. Borgs M, Bollen M, Keppens S, Yap SH, Stalmans W, Vanstapel F. Modulation of basal hepatic glycogenolysis by nitric oxide. Hepatology 1996;23:1564–1571
28. Sprangers F, Sauerwein HP, Romijn JA, van Woerkom GM, Meijer AJ. Nitric oxide inhibits glycogen synthesis in isolated rat hepatocytes. Biochem J 1998;330(Pt 2):1045–1049
29. Garthwaite J, Southam E, Boulton CL, Nielsen EB, Schmidt K, Mayer B. Potent and selective inhibition of nitric oxide-sensitive guanylyl cyclase by 1H-(1,2,4)oxadiazolo[4,3-a]quinoxalin-1-one. Mol Pharmacol 1995;48:184–188
30. Mannick JB, Miao XQ, Stamler JS. Nitric oxide inhibits Fas-induced apoptosis. J Biol Chem 1997;272:24125–24128
31. An Z, Winnick JJ, Farmer B, Lautz M, Neal D, Snead W, Cherrington AD. The cGMP pathway plays a role in the regulation of net hepatic glucose uptake (NHGU) in conscious dogs. Diabetes 2010;59:A412
32. Vaandrager AB, de Jonge HR. Signalling by cGMP-dependent protein kinases. Mol Cell Biochem 1996;157:23–30
33. Walter U. Distribution of cyclic-GMP-dependent protein kinase in various rat tissues and cell lines determined by a sensitive and specific radioimmunoassay. Eur J Biochem 1981;118:339–346
34. MacKenzie CJ, Wakefield JM, Cairns F, Dominiczak AF, Gould GW. Regulation of glucose transport in aortic smooth muscle cells by cAMP and cGMP. Biochem J 2001;353:513–519
35. Exton JH. Mechanisms of hormonal regulation of hepatic glucose metabolism. Diabetes Metab Rev 1987;3:163–183
36. Hardie DG, Carling D, Carlson M. The AMP-activated/SNF1 protein kinase subfamily: metabolic sensors of the eukaryotic cell? Annu Rev Biochem 1998;67:821–855
37. Lira VA, Soltow QA, Long JH, Betters JL, Sellman JE, Criswell DS. Nitric oxide increases GLUT4 expression and regulates AMPK signaling in skeletal muscle. Am J Physiol Endocrinol Metab 2007;293:E1062–E1068
38. Zhang J, Xie Z, Dong Y, Wang S, Liu C, Zou MH. Identification of nitric oxide as an endogenous activator of the AMP-activated protein kinase in vascular endothelial cells. J Biol Chem 2008;283:27452–27461
39. Ramnanan CJ, McMullen DC, Groom AG, Storey KB. The regulation of AMPK signaling in a natural state of profound metabolic rate depression. Mol Cell Biochem 2010;335:91–105
40. Viollet B, Foretz M, Guigas B, Horman S, Dentin R, Bertrand L, Hue L, Andreelli F. Activation of AMP-activated protein kinase in the liver: a new strategy for the management of metabolic hepatic disorders. J Physiol 2006;574:41–53
41. Bergeron R, Previs SF, Cline GW, Perret P, Russell RR 3rd, Young LH, Shulman GI. Effect of 5-aminoimidazole-4-carboxamide-1-beta-D-ribofuranoside infusion on in vivo glucose and lipid metabolism in lean and obese Zucker rats. Diabetes 2001;50:1076–1082
42. Foretz M, Ancellin N, Andreelli F, Saintillan Y, Grondin P, Kahn A, Thorens B, Vaulont S, Viollet B. Short-term overexpression of a constitutively active form of AMP-activated protein kinase in the liver leads to mild hypoglycemia and fatty liver. Diabetes 2005;54:1331–1339
43. Andreelli F, Foretz M, Knauf C, Cani PD, Perrin C, Iglesias MA, Pillot B, Bado A, Tronche F, Mithieux G, Vaulont S, Burcelin R, Viollet B. Liver adenosine monophosphate-activated kinase-α2 catalytic subunit is a key target for the control of hepatic glucose production by adiponectin and leptin but not insulin. Endocrinology 2006;147:2432–2441
44. Iglesias MA, Ye JM, Frangioudakis G, Saha AK, Tomas E, Ruderman NB, Cooney GJ, Kraegen EW. AICAR administration causes an apparent enhancement of muscle and liver insulin action in insulin-resistant high-fat-fed rats. Diabetes 2002;51:2886–2894
45. Camacho RC, Pencek RR, Lacy DB, James FD, Donahue EP, Wasserman DH. Portal venous 5-aminoimidazole-4-carboxamide-1-β-D-ribofuranoside infusion overcomes hyperinsulinemic suppression of endogenous glucose output. Diabetes 2005;54:373–382
46. Pencek RR, Shearer J, Camacho RC, James FD, Lacy DB, Fueger PT, Donahue EP, Snead W, Wasserman DH. 5-Aminoimidazole-4-carboxamide-1-β-D-ribofuranoside causes acute hepatic insulin resistance in vivo. Diabetes 2005;54:355–360
47. Polekhina G, Gupta A, Michell BJ, van Denderen B, Murthy S, Feil SC, Jennings IG, Campbell DJ, Witters LA, Parker MW, Kemp BE, Stapleton D. AMPK β subunit targets metabolic stress sensing to glycogen. Curr Biol 2003;13:867–871
48. Mukhtar MH, Payne VA, Arden C, Harbottle A, Khan S, Lange AJ, Agius L. Inhibition of glucokinase translocation by AMP-activated protein kinase is associated with phosphorylation of both GKRP and 6-phosphofructo-2-kinase/fructose-2,6-bisphosphatase. Am J Physiol Regul Integr Comp Physiol 2008;294:R766–R774